

## FULL PAPER

# Reduced graphene oxide/iron oxide hybrid composite material as an efficient magnetically separable heterogeneous catalyst for transfer hydrogenation of ketones

Samim Sultana<sup>1</sup> | Shreemoyee Bordoloi<sup>1,2</sup> | Surajit Konwer<sup>1</sup> |  
Geetika Borah<sup>1</sup> | Pradip K. Gogoi<sup>1</sup>

<sup>1</sup>Department of Chemistry, Dibrugarh University, Dibrugarh, 786004 Assam, India

<sup>2</sup>Department of Chemistry, MDKG College, Dibrugarh, 786004, India

## Correspondence

Surajit Konwer, Geetika Borah and Pradip K. Gogoi, Department of Chemistry, Dibrugarh University, Dibrugarh 786004, Assam, India.

Email: surajitkonwer@dibru.ac.in, geetikachem@yahoo.co.in, dr.pradip54@gmail.com

## Funding information

UGC-Maulana Azad National Fellowship, Delhi; DST-SERB, India; Sophisticated Test and Instrumentation Centre

Reduced graphene oxide was synthesized and functionalized with FeSO<sub>4</sub>·7H<sub>2</sub>O to form a reduced graphene oxide/iron oxide hybrid composite. The hybrid composite was extensively characterized using various techniques. Its application for transfer hydrogenation of various ketones was studied. The investigation showed that it serves as a good catalyst for transfer hydrogenation of aromatic and some aliphatic ketones resulting in excellent isolated yields (97–99%) of products. It is magnetically separable showing good reusability. The products were characterized and compared with authentic ones.

## KEYWORDS

aliphatic, aromatic, composite, reduced graphene oxide, transfer hydrogenation

## 1 | INTRODUCTION

Over the last few years, graphene oxide (GO) has been considered as an attractive supporting material for the heterogenization of catalysts because of its high surface area, edge reactivity, excellent thermal, mechanical and electrical properties and chemical stability,<sup>[1]</sup> and most significantly GO has a unique two-dimensional structure with numerous oxygen-containing functional groups, i.e. hydroxyl, epoxy, carboxyl and carbonyl groups.<sup>[2]</sup> Due to the presence of oxygenated functional groups on the GO surface, they can easily bind with metals and serve as activation sites for the growth of crystals onto the surface of GO.<sup>[3–6]</sup> In addition, the combination of GO and metals (like iron) can create new micropores at the interface of both components, which improve the accessibility of reactants to the active sites and therefore reduce the mass-transfer-limitation effects during catalysis.<sup>[5,6]</sup>

Furthermore, GO is able to promote the internal electron transfer process in such composites and induce a synergistic effect between both components to improve catalytic activity.<sup>[3,5,7,8]</sup>

The combination of reduced GO (rGO) with iron oxide nanocomposites has attracted the interest of the scientific community as promising materials for catalysis because such combination allows adsorption through  $\pi$ - $\pi$  conjugation. In addition the unique surface properties of rGO allow it to accept electrons to hinder the recombination of photo-induced electrons and holes.<sup>[9]</sup> Though iron oxide is a significant transition metal oxide that has been extensively used as a catalyst in various fields, the catalytic activity is not so satisfactory because of aggregation which greatly decreases the surface area. Therefore the intercalation of iron oxide into rGO may solve this problem by enhancing the properties especially in the field of catalysis.<sup>[10]</sup>

Transfer hydrogenation of ketones to their corresponding alcohols catalyzed by transition metal complexes is an interesting research area in modern synthetic chemistry. It is a powerful and convenient route for reducing carbonyl compounds without the use of hazardous hydrogen gas or moisture-sensitive hydride reagents under mild reaction condition and hence is considered as an alternative to direct hydrogenation.<sup>[11-16]</sup> Nowadays, the synthesis of chiral alcohols, important intermediates for the synthesis of chiral drugs and fine chemicals, is indispensable,<sup>[17]</sup> and hence discovering green and effective approaches for the synthesis of chiral alcohols is of great concern, transfer hydrogenation of ketones being one of them. Transfer hydrogenation reactions are environmentally benign and sustainable compared to catalytic hydrogenation reactions (using molecular hydrogen and high pressure) as there is no generation of hazardous wastes at the end of the reaction and the use of suitable hydrogen donors control the reaction rate and selectivity of the reaction.<sup>[18]</sup> Commonly used hydrogen donors are formic acid, aqueous sodium formate, azeotropic mixtures of formic acid/triethylamine and 2-propanol,<sup>[19]</sup> but 2-propanol is mostly used as hydrogen donor because it is inexpensive, safe, non-toxic and environment friendly.<sup>[20]</sup> Generally, in academic and industrial operations, noble, precious and highly toxic metals such as Pd,<sup>[21]</sup> Rh,<sup>[22,23]</sup> Ru<sup>[17,24-29]</sup> and Ir<sup>[30]</sup> are typically used for transfer hydrogenation reactions. Therefore, in recent years, transfer hydrogenation reactions using abundant and environmentally benign metals such as Fe, Co, Ni, etc., replacing the precious and highly toxic metals are gaining much attention.<sup>[31]</sup> Transfer hydrogenation reactions of ketones using Fe,<sup>[32]</sup> Mn<sup>[33]</sup> and Mo<sup>[34]</sup> have also been reported.

Hence, in continuation of our previous work on heterogeneous catalysis,<sup>[32,35]</sup> we are interested in developing a simple, environmentally benign protocol for transfer hydrogenation of ketones catalyzed by such eco-friendly and nontoxic metals. Herein, we report the synthesis and characterization of rGO/iron oxide hybrid composite material and its application in transfer hydrogenation of ketones.

## 2 | EXPERIMENTAL

### 2.1 | Materials

Chemical reagents such as sulfuric acid (H<sub>2</sub>SO<sub>4</sub>, 98%), sodium nitrate (NaNO<sub>3</sub>), potassium permanganate (KMnO<sub>4</sub>, 99.9%), hydrogen peroxide (H<sub>2</sub>O<sub>2</sub>, 30%), iron(II) sulfate (FeSO<sub>4</sub>·7H<sub>2</sub>O, 99.5%) and ammonium

hydroxide (NH<sub>4</sub>OH, 25%) were of analytical reagent grade and used as received. Graphite flakes were purchased from Shanker Graphites and Chemical, New Delhi, India. For all purposes, double-distilled water was used.

2-Propanol, sodium hydroxide and potassium hydroxide were procured from Merck. Acetophenone, 4-hydroxy acetophenone, 4-chloro acetophenone, 4-nitro acetophenone, 4-bromo acetophenone, benzophenone, 4-bromo benzophenone, 2-pentanone, 3-pentanone and cyclohexanone were obtained from Tokyo Chemical Industry. All the reagents were of analytical reagent grade and used as received without further purification.

### 2.2 | Preparation of GO

GO was synthesized from graphite by adopting a simplified Hummers method as reported elsewhere.<sup>[36]</sup> Here graphite powder (3 g) was treated with H<sub>2</sub>SO<sub>4</sub> (120 ml) and NaNO<sub>3</sub> (2.5 g) followed by addition of KMnO<sub>4</sub> (15 g) with vigorous stirring maintaining the temperature at less than 20°C. To ensure complete oxidation of the graphite, the solution was stirred at room temperature for more than 24 hours. Then water (150 ml) was added slowly with vigorous agitation at 98°C for one day, and finally H<sub>2</sub>O<sub>2</sub> (50 ml) solution was added to stop the oxidation process, during which the color of the solution become bright yellow, indicating the highly oxidized level of the graphite. The resulting GO was washed by rinsing and centrifugation with an aqueous solution containing 1 M HCl followed by deionized water several times. After filtration and drying under vacuum, the GO was obtained as grey powder.

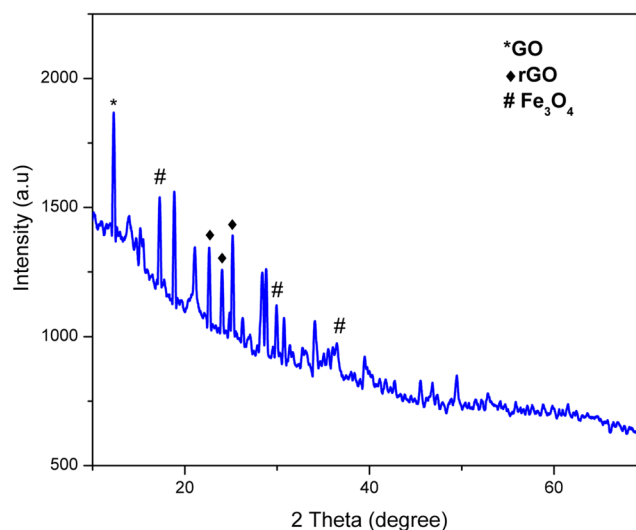


FIGURE 1 XRD pattern of rGO/Fe<sub>3</sub>O<sub>4</sub> composite

### 2.3 | Preparation of rGO/iron oxide (rGO/Fe<sub>3</sub>O<sub>4</sub>) composite

The rGO/Fe<sub>3</sub>O<sub>4</sub> composite was prepared using a simple *in situ* chemical synthesis method. A mixture of GO (200 mg) and deionized double-distilled water (50 ml) in a round-bottom flask was subjected to

ultrasonication about 30 minutes. To this dispersed solution, FeSO<sub>4</sub>·7H<sub>2</sub>O (50 mg) was added and the mixture was stirred for 24 hours at room temperature. To this mixture, 2 ml of 25% ammonium hydroxide was added dropwise to maintain the pH at 8. Upon addition of ammonium hydroxide, the color of the mixture turned reddish and finally became a deep red color

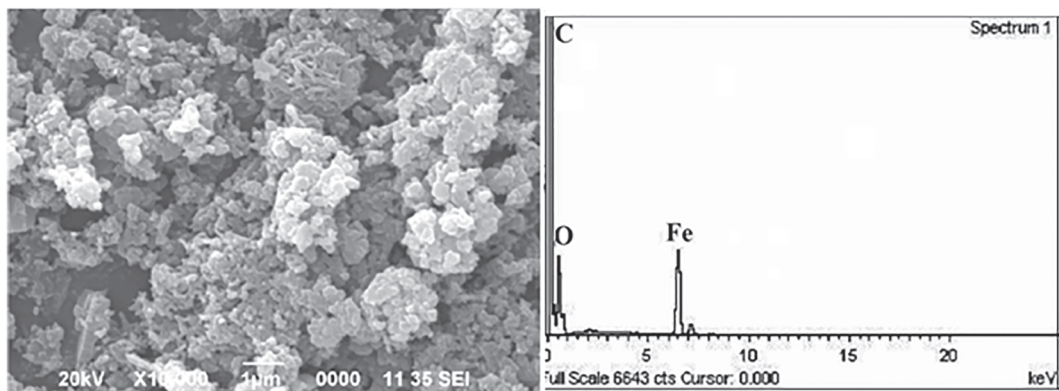


FIGURE 2 SEM image and energy-dispersive X-ray spectrum of rGO/Fe<sub>3</sub>O<sub>4</sub>

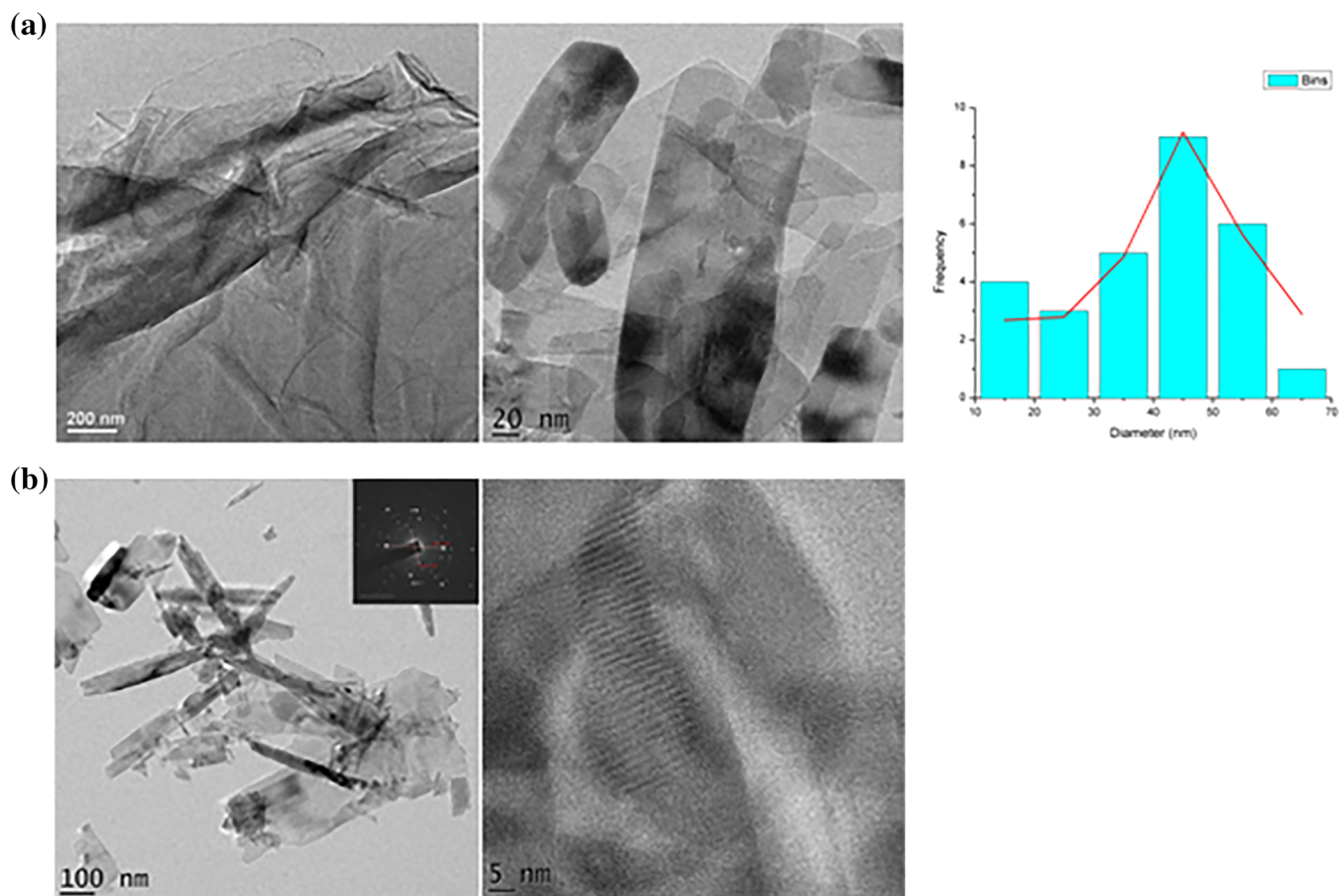


FIGURE 3 (a) TEM images of GO and rGO/Fe<sub>3</sub>O<sub>4</sub> composite. (b) High-resolution TEM images of rGO/Fe<sub>3</sub>O<sub>4</sub> composite with selected area electron diffraction pattern (inset)

because of the formation of ferric hydroxide. Then 0.7 ml of hydrazine hydrate was added dropwise and the mixture was kept for 24 hours at *ca* 90°C. The resulting mixture was finally washed with ethanol and water and then dried in a vacuum oven at 60°C.

## 2.4 | General characterization

Fourier transform infrared (FT-IR) spectroscopy was conducted with an Impact 410 (Nicolet, USA), using KBr pellets (400–4000  $\text{cm}^{-1}$ ). Scanning electron microscopy (SEM) images were recorded using a JSM-6390LV (JEOL, Japan) at 20 kV. TEM images were recorded at STIC Cochin and SAIC, Tezpur University using a Jeol/JEM 2100 and Tecnai G2 20 S-Twin (200 kV), at a resolution of 2.4 Å, respectively. A powder X-ray diffraction (XRD) study was carried out at room temperature (*ca* 25°C) using a Rigaku X-ray diffractometer with Cu K $\alpha$  radiation ( $\lambda = 0.15418$  nm) at 30 kV and 15 mA using a scanning rate of 0.050°  $\text{s}^{-1}$  in the range  $2\theta = 10\text{--}70^\circ$ . X-ray photoelectron spectroscopy (XPS) was performed at ACMS, IIT Kanpur with an XPS-AES Module, model PHI 5000 Versa Prob II (FEI Inc.). Gas chromatography–mass spectrometry (GC–MS) analysis of the products was conducted using an Agilent Technologies GC system (7820) coupled with a mass detector (5975) and SHRXI-5MS column.  $^1\text{H}$  NMR spectra of the products were recorded in  $\text{CDCl}_3$  using a JEOL ECS-400. The magnetic hysteresis behavior of as-synthesized rGO/ $\text{Fe}_3\text{O}_4$  composite material was investigated at room temperature against variable field using a Lakeshore 7410 series magnetometer.

## 2.5 | General procedure for transfer hydrogenation of ketones using rGO/ $\text{Fe}_3\text{O}_4$ composite material as catalyst

The transfer hydrogenation reaction was carried out taking ketone (1 mmol), rGO/ $\text{Fe}_3\text{O}_4$  composite catalyst (10 mg, 6.1 mol% of Fe), *i*-PrOH (5 ml) and Na-*i*-OPr (5 ml) in a round-bottomed flask and refluxing at 80°C for the required amount of time. The progress of the reaction was monitored continuously using TLC with 5% ethyl acetate–hexane. At the completion of the reaction (monitored using GC–MS), stirring was stopped and the catalyst was separated from the reaction mixture using a magnet. The remaining reaction mixture was diluted with water (10 ml) and then extracted with ethyl acetate (10 ml). The combined

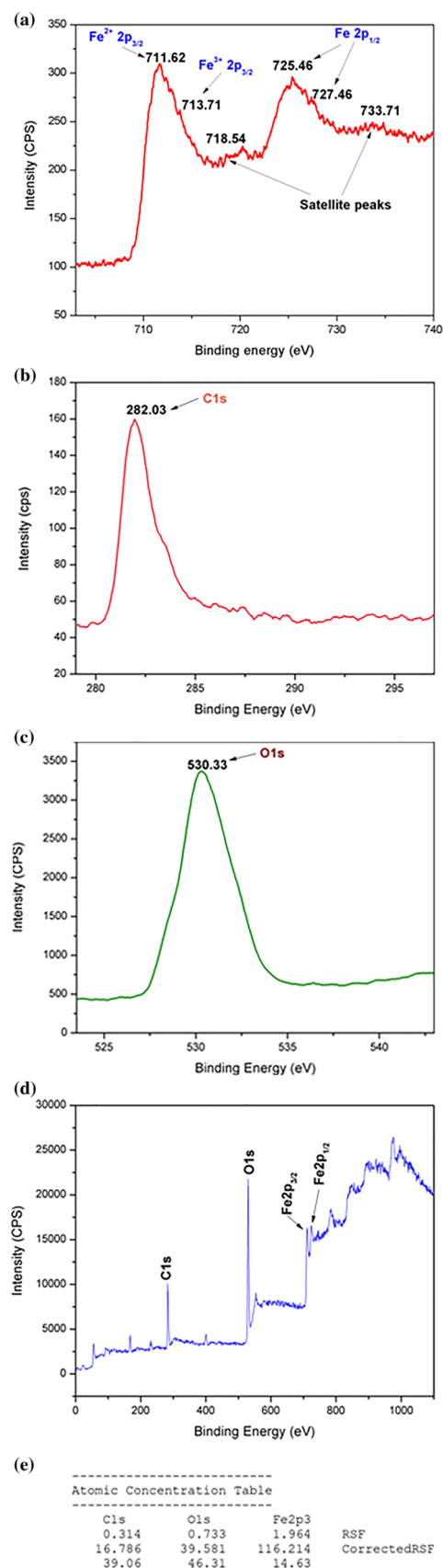


**FIGURE 4** XPS spectra of rGO/ $\text{Fe}_3\text{O}_4$  composite for (a) Fe 2p<sub>3/2</sub>, (b) C 1s, (c) O 1s and (d) Fe 2p<sub>3/2</sub>, C 1s and O 1s together. (e) Quantitative analysis

extract was washed with brine and dehydrated over anhydrous  $\text{Na}_2\text{SO}_4$ . It was then purified by column chromatography (silica gel chromatography using ethyl acetate–hexane, 5:95) to afford the desired pure products. For recycling of the catalyst, after completion of the reaction the catalyst was isolated from the reaction mixture using a magnet and washed several times with water and ethyl acetate after each cycle. It was then dried at  $110^\circ\text{C}$  in an oven overnight. The recovered catalyst was subjected to subsequent runs under the same reaction conditions.

### 3 | RESULTS AND DISCUSSION

#### 3.1 | Preparation of composite

The brownish-grey GO is mainly composed of carbon and oxygen with a C:O ratio of between 2.1 and 2.9 and it consists of loosely bound carbon layers. The surface of the GO sheet is bonded with various oxygen-containing functional groups, i.e. carboxyl, hydroxyl, etc., due to which it forms a stable aqueous suspension upon ultrasonication and stirring. Moreover, the oxygen-containing functional groups can be used to cross-link carbon with iron compounds to form the  $\text{rGO}/\text{Fe}_3\text{O}_4$  composite.<sup>[37]</sup>

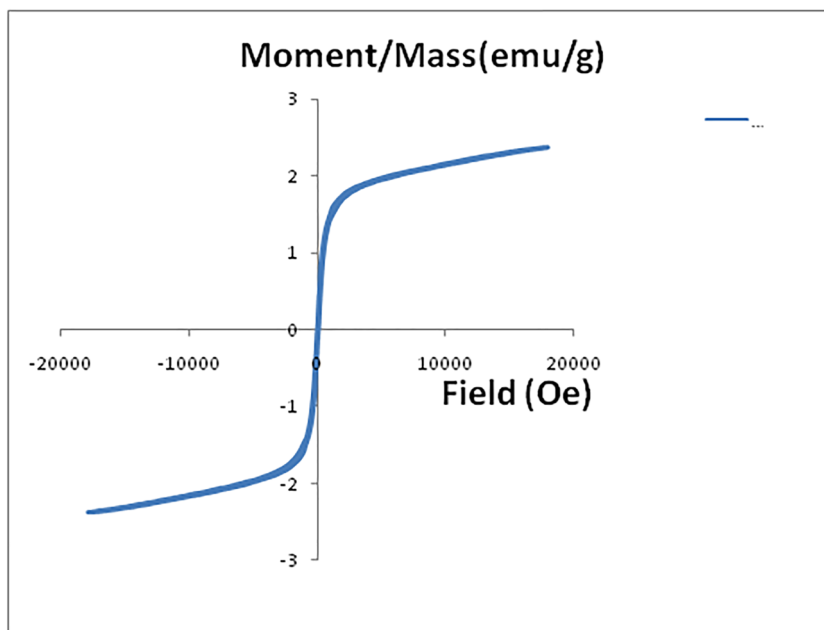
#### 3.2 | Characterization of composite

##### 3.2.1 | FT-IR study

In the FT-IR spectrum of GO (Figure S1a), the peaks at  $3434\text{ cm}^{-1}$  (broad) and  $1730\text{ cm}^{-1}$  correspond to the O–H and C=O stretching vibrations, respectively. The peaks at  $1222$  and  $1485\text{ cm}^{-1}$  could be assigned to the C–O–C and C–OH stretching vibrations, respectively.<sup>[38]</sup> The band at  $1077\text{ cm}^{-1}$  corresponds to the C–O stretching vibration, indicating the presence of epoxide group in the GO layers. In the FT-IR spectrum of the  $\text{rGO}/\text{Fe}_3\text{O}_4$  composite (Figure S1b), the peaks at  $3159$ ,  $3093$ ,  $1520$  and  $1100\text{ cm}^{-1}$  could be attributed to the O–H, C–H, C–OH and C–O stretching vibrations, respectively. The broad peak at about  $707\text{ cm}^{-1}$  could be due to stretching of Fe–O bond in bulk  $\text{Fe}_3\text{O}_4$  indicating that  $\text{Fe}_3\text{O}_4$  is bound to –COO on the GO surface, while that at  $561\text{ cm}^{-1}$  might be assigned to the Fe–O bending vibration resulting from the formation of the  $\text{rGO}/\text{Fe}_3\text{O}_4$  composite.<sup>[39,40]</sup>

##### 3.2.2 | XRD analysis

Figure 1 depicts a representative XRD pattern of the  $\text{rGO}/\text{Fe}_3\text{O}_4$  composite, which coincides with the results from the TEM images (Figure 3) and supporting the formation of crystalline  $\text{rGO}/\text{iron oxide}$  (i.e.  $\text{Fe}_3\text{O}_4$ )



Coercivity (Hci)	53.476 Oe
Magnetization (Ms)	2.3780 emu/g
Retentivity (Mr)	0.12777 emu/g

FIGURE 5 Magnetic hysteresis loop of  $\text{rGO}/\text{Fe}_3\text{O}_4$

composite. The XRD pattern of the composite displays a series of diffraction peaks at  $2\theta = 17.21^\circ$ ,  $30.85^\circ$  and  $36.55^\circ$  due to (111), (220) and (311) crystal planes of cubic spinel structure of magnetite  $\text{Fe}_3\text{O}_4$ .<sup>[41]</sup> The sharp peak at  $2\theta$  of  $12.28^\circ$  is the characteristic peak of GO, while the peaks at  $2\theta$  of  $22.65^\circ$ ,  $24.05^\circ$  and  $25.16^\circ$  could be assigned to rGO.<sup>[42–44]</sup>

### 3.2.3 | SEM analysis

In the SEM micrographs of the rGO/ $\text{Fe}_3\text{O}_4$  composite (Figure 2), smooth surfaces are observed. Since the iron particles are grown in the pores and galleries of GO sheets, the identification of individual phases is difficult from the SEM micrograph. However, from the energy-dispersive X-ray spectrum of the composite, the presence of a high level of iron particles with oxygen molecules is

observed which indicates the homogeneous distribution of iron oxide onto GO sheets. This structure enables a good connection and intimate contact between the components.

### 3.2.4 | TEM analysis

The morphologies of GO and rGO/ $\text{Fe}_3\text{O}_4$  composite are shown in TEM images (Figure 3a) along with particle size distribution. The as-prepared rGO/ $\text{Fe}_3\text{O}_4$  has a typically curved, layer-like structure with average sheet thickness of 40–50 nm. For the rGO/ $\text{Fe}_3\text{O}_4$  composite, the high-resolution TEM images (Figure 3b) show that all the GO sheets are homogeneously coated with iron oxide particles that are mainly grown on the surface or intercalate between the rGO sheets. SEM and TEM images reveal the uniform adsorption of iron oxide particles onto the

**TABLE 1** Optimization of reaction conditions for transfer hydrogenation of benzophenone using rGO/ $\text{Fe}_3\text{O}_4$  composite catalyst<sup>a</sup>

Entry	Catalyst (mol% of Fe)	Hydrogen donor	Base	Time (h)	Isolated yield (%)
1	—	<i>i</i> -PrOH	KOH	24	—
2	3.05 in 5 mg	<i>i</i> -PrOH	—	24	—
3	3.05 in 5 mg	<i>i</i> -PrOH	K- <i>i</i> -OPr	24	—
4	6.1 in 10 mg	<i>i</i> -PrOH	K- <i>i</i> -OPr	24	—
5	9.15 in 15 mg	<i>i</i> -PrOH	K- <i>i</i> -OPr	24	—
6	12.2 in 20 mg	<i>i</i> -PrOH	K- <i>i</i> -OPr	24	—
7	12.2 in 20 mg	<i>i</i> -PrOH	KOH	24	— <sup>b</sup>
8	3.05 in 5 mg	<i>i</i> -PrOH	K- <i>i</i> -OPr	5	63 <sup>b</sup>
9	6.1 in 10 mg	HCOOH	K- <i>i</i> -OPr	6	— <sup>c</sup>
10	12.2 in 20 mg	HCOOH	Et <sub>3</sub> N	6	— <sup>c</sup>
11	12.2 in 20 mg	HCOOH	Et <sub>3</sub> N	6	— <sup>d</sup>
12	3.05 in 5 mg	<i>i</i> -PrOH	K- <i>i</i> -OPr	3	86 <sup>d</sup>
13	6.1 in 10 mg	<i>i</i> -PrOH	K- <i>i</i> -OPr	3	86 <sup>d</sup>
14	12.2 in 20 mg	<i>i</i> -PrOH	K- <i>i</i> -OPr	3	86 <sup>d</sup>
<b>15</b>	<b>6.1 in 10 mg</b>	<b><i>i</i>-PrOH</b>	<b>Na-<i>i</i>-OPr</b>	<b>3</b>	<b>99<sup>d</sup></b>
16	9.15 in 15 mg	<i>i</i> -PrOH	Na- <i>i</i> -OPr	3	99 <sup>d</sup>
17	12.2 in 20 mg	<i>i</i> -PrOH	Na- <i>i</i> -OPr	3	99 <sup>d</sup>

<sup>a</sup>Reaction conditions: benzophenone (1 mmol), hydrogen donor (5 ml), base (2 mmol or 5 ml Na-*i*-OPr/K-*i*-OPr prepared by refluxing 2 mmol of base in 20 ml of *i*-PrOH), catalyst (rGO/ $\text{Fe}_3\text{O}_4$ ), room temperature (25°C) in air unless otherwise noted.

<sup>b</sup>At 60°C.

<sup>c</sup>At 70°C.

<sup>d</sup>At 80°C.

chemically modified rGO surface and/or filled between the rGO nanosheets.

### 3.2.5 | XPS analysis

In the XPS spectrum of the composite (Figure 4a), two peaks at binding energies of 711.62 and 713.71 eV correspond to  $\text{Fe}^{2+} 2p_{3/2}$  and  $\text{Fe}^{3+} 2p_{3/2}$ , respectively, which are indicative of structural configuration of  $\text{Fe}_3\text{O}_4$ . Two satellite peaks at 718.54 and 733.71 eV confirm that the Fe in the composite is in the divalent state. In addition, peaks at 725.46 and 727.46 eV corresponding to Fe  $2p_{1/2}$  of Fe are also observed. The XPS spectra for C 1s (Figure 4b) and O 1s (Figure 4c) are also shown. For O 1s, a peak at binding energy of 530.33 eV is observed which is the typical state of Fe–O corresponding to  $\text{Fe}_3\text{O}_4$ .<sup>[45,46]</sup>

### 3.2.6 | Vibrating sample magnetometry

The room temperature magnetic hysteresis behavior (magnetization and field) of  $\text{rGO}/\text{Fe}_3\text{O}_4$  shown in Figure 5 was studied using a vibrating sample magnetometer. It exhibited a characteristic pattern of a ferromagnetic component. As the driving magnetic field was decreased to zero, the composite had still a remanence value of  $0.128 \text{ emu g}^{-1}$  with coercivity value of  $53.476 \text{ Oe}$ . The saturation magnetization was found to be  $2.3780 \text{ emu g}^{-1}$ . This behavior of the synthesized material unambiguously supports the presence of a ferromagnetic component.

## 3.3 | Transfer hydrogenation of ketones catalyzed by $\text{rGO}/\text{Fe}_3\text{O}_4$ composite material

To optimize the reaction conditions such as temperature, reaction time, catalyst loading, base, etc., for excellent catalytic performance, a number of runs were carried out using benzophenone as the starting substrate (Table 1). Initially, benzophenone (1 mmol), *i*-PrOH (5 ml) and KOH (2 mmol) were taken in the absence of the catalyst and stirred for 24 hours at room temperature, which resulted in no product formation (Table 1, entry 1). In the next move, 5 mg of  $\text{rGO}/\text{Fe}_3\text{O}_4$  composite catalyst (3.05 mol% of Fe) was introduced in the absence of any base followed by stirring for 24 hours (Table 1, entry 2), which also showed no product formation. This clearly shows the importance of both catalyst and base for the reaction to proceed. It has been observed that using *K-i*-OPr (base) and *i*-PrOH (hydrogen donor) at  $60^\circ\text{C}$  results in 63% product formation (Table 1, entry 8), while raising temperature to  $80^\circ\text{C}$  afforded 86% product formation, which does not increase further even on increasing the amount of the catalyst (Table 1, entries 12–14). But use of *Na-i*-OPr (base) in *i*-PrOH (hydrogen donor) at  $80^\circ\text{C}$  gives the best result within 3 hours (99%) (Table 1, entry 15). Hence, after careful investigation of a wide range of catalytic reaction parameters, 10 mg of the  $\text{rGO}/\text{Fe}_3\text{O}_4$  composite catalyst (6.1 mol% of Fe), *Na-i*-OPr in *i*-PrOH at  $80^\circ\text{C}$  seemed the most suitable for further catalytic reactions.

Since the role of base is very important in transfer hydrogenation of benzophenone, we investigated the

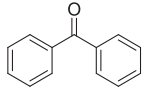
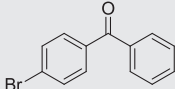
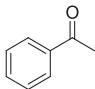
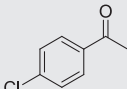
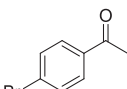
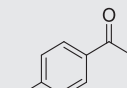
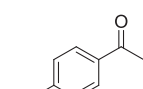
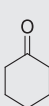
**TABLE 2** Optimization of base for transfer hydrogenation of benzophenone<sup>a</sup>

Entry	Base	Isolated yield (%)
1	KOH	—
2	<i>K-i</i> -OPr	86 <sup>b</sup>
3	NaOH	—
4	<i>Na-i</i> -OPr	93
5	<b><i>Na-i</i>-OPr</b>	<b>99<sup>b</sup></b>
6	$\text{Na}_2\text{CO}_3$	—
7	$\text{Et}_3\text{N}$	—
8	$\text{NaHCO}_3$	—
9	$\text{K}_2\text{CO}_3$	—

<sup>a</sup>Reaction conditions: benzophenone (1 mmol), hydrogen donor (*i*-PrOH, 5 ml), base (1 mmol), catalyst ( $\text{rGO}/\text{Fe}_3\text{O}_4$  composite, 6.1 mol% of Fe, 10 mg),  $80^\circ\text{C}$ .

<sup>b</sup>2 mmol of base.

**TABLE 3** Transfer hydrogenation of various substrates using rGO/Fe<sub>3</sub>O<sub>4</sub> composite catalyst<sup>a</sup>

Entry	Substrate	Time (h)	Isolated yield (%)	Conversion (GC-MS) (%)	TON	TOF ( $\times 10^{-3} \text{ h}^{-1}$ )
1		3	99	100	16.23	5410
2		2	99	100	16.23	8115
3		2.5	99	100	16.23	6492
4		2	97	100	15.9	7951
5		2	98	99	16.06	8033
6		3	—	—	—	—
7		3	—	—	—	—
8		3	99	100	16.23	5410

(Continues)



TABLE 3 (Continued)

Entry	Substrate	Time (h)	Isolated yield (%)	Conversion (GC-MS) (%)	TON	TOF ( $\times 10^{-3} \text{ h}^{-1}$ )
9		3	—	—	—	—
10		3	—	—	—	—

<sup>a</sup>Reaction conditions: ketone (1 mmol), *i*-PrOH (5 ml), Na-*i*-OPr (5 ml), rGO/Fe<sub>3</sub>O<sub>4</sub> composite (10 mg, 6.1 mol% of Fe) at 80°C in air. Formation of products was confirmed using FT-IR, <sup>1</sup>H NMR and GC-MS analyses and then compared authentically. TON, turnover number; TOF, turnover frequency.

reaction using bases such as KOH, K-*i*-OPr, NaOH, Na-*i*-OPr, Na<sub>2</sub>CO<sub>3</sub>, Et<sub>3</sub>N, NaHCO<sub>3</sub> and K<sub>2</sub>CO<sub>3</sub> (Table 2) and observed that 2 mmol of Na-*i*-OPr gives best result at 80 C in 3 hours (Table 2, entry 5).

With the optimized reaction conditions (i.e. 10 mg of rGO/Fe<sub>3</sub>O<sub>4</sub> composite as catalyst, 5 ml of *i*-PrOH as hydrogen donor and 5 ml of Na-*i*-OPr as the base at 80 C for 3 hours) in hand, we studied the scope and efficiency of this methodology and hence employed various substrates to investigate the scope of the catalyst (Table 3). It was observed that hydrogenation of benzophenone (Table 3, entry 1) is slower than that of acetophenone (Table 3, entry 3) which may be attributed to increased ring strain due to two bulky phenyl rings in the benzophenone substrate.<sup>[47]</sup> 4-Bromo benzophenone (Table 3, entry 2) gives a better result than benzophenone which may be due to the electron-withdrawing effect of Br at *p*-position. A similar effect is also observed in the case of 4-chloro acetophenone and 4-bromo acetophenone (Table 3, entries 4 and 5) which reduces the electron density on the carbonyl group increasing the affinity of the substrates towards easier hydrogenation. On the other hand, 4-hydroxy acetophenone (Table 3, entry 6) with its electron-donating OH group decelerates the reaction resulting in no product formation.<sup>[24]</sup> 4-Nitro acetophenone (Table 3, entry 7)<sup>[48]</sup> and aliphatic substrates (Table 3, entries 9–15) except cyclohexanone (Table 3, entry 8)<sup>[13]</sup> were difficult to reduce using our catalyst.

It is pertinent to mention that a comparative study was carried out of various Fe-based catalysts for transfer hydrogenation of carbonyl compounds (Table 4), and it was observed that in most cases high temperature or

inert atmosphere were used and afforded highest isolated yield of 99% with 3–6 reuse cycles. However, our rGO/Fe<sub>3</sub>O<sub>4</sub> composite catalyst gave 97–99% isolated yield at 80°C. Moreover, our catalyst could be easily separated from the reaction mixture using a magnet and reused for at least five times without compromising its activity. To the best of our knowledge, our rGO/Fe<sub>3</sub>O<sub>4</sub> composite material system represents one of the best magnetically recyclable catalytic systems reported so far for transfer hydrogenation of ketones. Hence, the results in Table 4 show the superior efficacy of our catalyst over other previously reported Fe-based catalysts.

### 3.3.1 | Probable mechanism

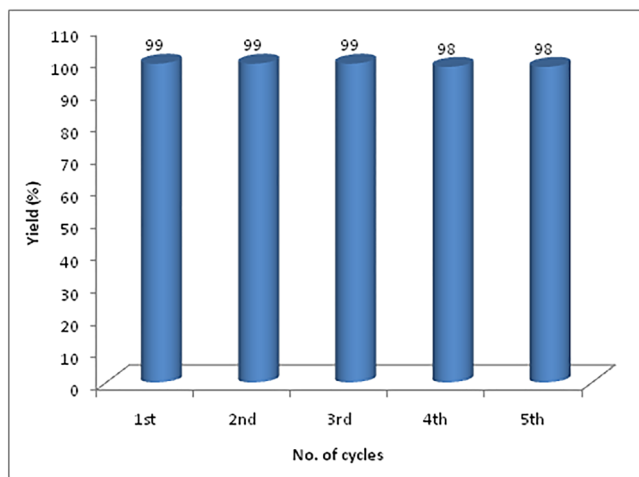
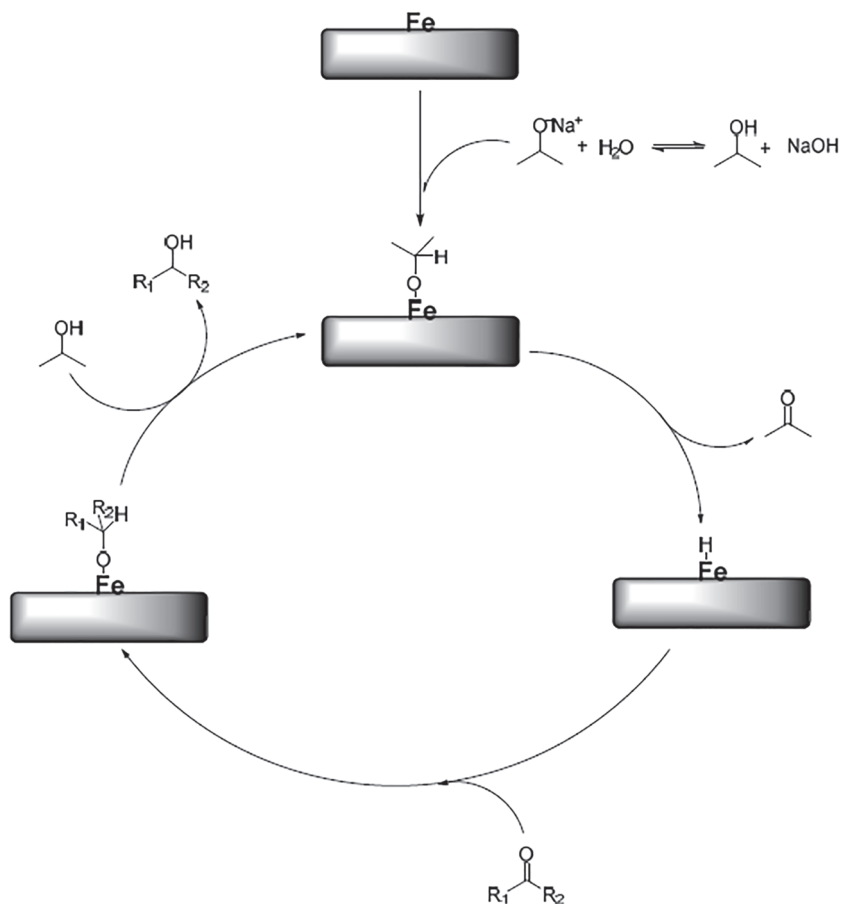
A plausible mechanism for hydrogenation of ketones<sup>[56,57]</sup> using the rGO/Fe<sub>3</sub>O<sub>4</sub> catalyst is demonstrated in Scheme 1.

### 3.3.2 | Catalyst recycling

The most important advantage of immobilized complexes is their recyclability. In order to study its sustainability, recyclability of the catalyst was investigated using benzophenone as the model substrate. At reaction completion, the catalyst was easily separated from the reaction mixture using a magnet, washed several times with distilled water, dried and reused in a subsequent reaction. To our delight, the catalyst could be recycled at least five times without compromising its catalytic efficiency or product yield (Figure 6).

TABLE 4 Comparative study

Entry	Catalyst	Reactants	Temperature (°C); reaction conditions	Reaction time (reusability)	Solvent	Isolated yield (%)	Ref.
1	rGO/Fe <sub>3</sub> O <sub>4</sub> composite	Aromatic ketones with derivatives, cyclohexanone	80; Magnetic stirring	2–3 h (Magnetically separable; 5 cycles)	i-PrOH	97–99	This
2	Fe@imine-mont-K10	Both aromatic and aliphatic ketones	80; Magnetic stirring	30 min–5 h (5 cycles)	i-PrOH/CH <sub>3</sub> CN (1:1)	51–99	[31]
3	2-[1-(3,5-Dimethylpyrazol-1-yl) ethyl]pyridine Fe(II)Cl <sub>2</sub>	Acetophenone	82; Magnetic stirring	48 h	i-PrOH	67	[47]
4	FePc/Al <sub>2</sub> O <sub>3</sub>	Benzaldehyde, acetophenone and derivatives	80; Magnetic stirring	6–12 h (3 cycles)	i-PrOH	33–99	[49]
5	N-heterocyclic carbene iron(II) complexes	aromatic, cyclic and aliphatic ketones	82; Magnetic stirring, inert atmosphere	12 h	i-PrOH	3–87	[50]
6	Iron phthalocyanine, Fe(Pc)	<i>trans</i> -Cinnamaldehyde, benzaldehyde and derivatives	80; Magnetic stirring, Ar atmosphere	6 or 12 h (3 cycles)	i-PrOH	25–99	[51]
7	$\gamma$ -Fe <sub>2</sub> O <sub>3</sub> @HAP	Furfural, hydroxyl methylfurfural, ethyl levulinic, acetophenone, benzaldehyde	180; Magnetic stirring	10 h (6 cycles)	i-PrOH	80–95.3	[52]
8	(Pyrazole)pyridine iron(II)	Benzophenone, acetophenone and derivative, 2-methylcyclohexanone, 3-pentanone, 2-acetylpyridine	82; Magnetic stirring	48 h	i-PrOH	56–99	[53]
9	Nitrogen-doped carbon-supported iron catalyst	Furfural	180; Magnetic stirring	6 h (5 cycles)	i-PrOH	91.6	[54]
10	ImmFe-IL	Nitroarenes	110; Magnetic stirring	12 h (4 cycles)	Hydrazine hydrate and ethylene glycol	20–99	[55]

**SCHEME 1** Plausible mechanism for transfer hydrogenation of ketones**FIGURE 6** Recycling of the catalyst

## 4 | CONCLUSIONS

The present study reports the formulation of a new Fe-based hybrid composite material obtained by immobilization on synthesized GO. The composite material was found to be crystalline and showed excellent catalytic activity for transfer hydrogenation of ketones in *i*-PrOH. The advantages of the catalyst are that it is magnetically

separable and could be recycled at least five times without significant loss in activity.

## ACKNOWLEDGEMENTS

The authors thank STIC, Cochin for high-resolution TEM, IIT Kanpur for XPS, CIF, IIT Guwahati for vibrating sample magnetometry, and SAIC, Tezpur University for TEM and  $^1\text{H}$  NMR analytical facilities and UGC-SAP-DRS-I program (2016-2021). S.B. thanks DST-SERB, India for financial support of the research work under DST Women Scientist Scheme A (no. SR/WOS-A/CS-161/2016). S.S. is grateful to UGC-Maulana Azad National Fellowship, Delhi for financial support.

## DECLARATION OF INTEREST STATEMENT

The authors declare that there is no conflict of interest regarding the publication of this article.

## ORCID

Geetika Borah  <https://orcid.org/0000-0002-5781-1694>

## REFERENCES

- [1] H. Wang, H. S. Casalongue, Y. Liang, H. Dai, *J. Am. Chem. Soc.* **2010**, *132*, 7472.

- [2] D. R. Dreyer, S. Park, C. W. Bielawski, R. S. Ruoff, *Chem. Soc. Rev.* **2010**, *39*, 228.
- [3] Y. Zhang, G. Li, H. Lu, Q. Lv, Z. Sun, *RSC Adv.* **2014**, *4*, 7594.
- [4] R. Kumar, K. Jayaramulu, T. K. Maji, C. N. R. Rao, *Chem. Commun.* **2013**, *49*, 4947.
- [5] C. Petit, T. J. Bandosz, *Adv. Mater.* **2009**, *21*, 4753.
- [6] N. A. Zubir, C. Yacou, J. Motuzas, X. Zhang, X. S. Zhao, J. C. D. da Costa, *Chem. Commun.* **2015**, *51*, 9291.
- [7] M. Jahan, Q. Bao, J. X. Yang, K. P. Loh, *J. Am. Chem. Soc.* **2010**, *132*, 14487.
- [8] N. A. Zubir, C. Yacou, J. Motuzas, X. W. Zhang, J. C. D. da Costa, *Sci. Rep.* **2014**, *4*, 4594.
- [9] T. P. See, A. Pandikumar, L. H. Ngee, H. N. Ming, C. C. Hua, *Catal. Sci. Technol.* **2014**, *4*, 4396.
- [10] S. Paulose, R. Raghavan, B. K. George, *RSC Adv.* **2016**, *6*, 45977.
- [11] A. M. Pálvölgyi, J. Bitai, V. Zeindlhofer, C. Schröder, K. Bica, *ACS Sustainable Chem. Eng.* **2019**, *7*, 3414.
- [12] S. Biswas, D. Sarkar, P. Roy, T. K. Mondal, *Polyhedron* **2017**, *131*, 1.
- [13] L. Wang, T. Liu, *Chin. J. Catal.* **2018**, *39*, 327.
- [14] S. Biswas, P. Roy, S. Jana, T. K. Mondal, *J. Organometal. Chem.* **2017**, *846*, 201.
- [15] B. Stefane, F. Pozgan, *Catal. Rev. Sci. Eng.* **2014**, *56*, 82.
- [16] M. Aydemir, N. Meric, C. Kayan, F. Ok, A. Baysal, *Inorg. Chim. Acta* **2013**, *398*, 1.
- [17] G. Tang, M. Chen, J. Fang, Z. Xu, H. Gong, Q. Peng, Z. Hou, *Catal. Commun.* **2019**, *121*, 43.
- [18] A. Lazar, S. Silpa, C. P. Vinod, A. P. Singh, *Mol. Catal.* **2017**, *440*, 66.
- [19] T. M. Townsend, C. Kirby, A. Ruff, A. R. O'Connor, *J. Organometal. Chem.* **2017**, *843*, 7.
- [20] A. Matsunami, Y. Kayaki, *Tetrahedron Lett.* **2018**, *59*, 504.
- [21] T. Song, Y. Duan, Y. Yang, *Catal. Commun.* **2019**, *120*, 80.
- [22] P. Roy, C. K. Manna, R. Naskar, T. K. Mondal, *Polyhedron* **2019**, *158*, 208.
- [23] J. Li, J. Han, Z. Lin, L. Tang, Q. Huang, Q. Wang, J. Zhu, J. Deng, *Tetrahedron* **2019**, *75*, 422.
- [24] M. K. Yılmaz, M. Keleş, *Transit. Met. Chem.* **2018**, *43*, 285.
- [25] N. Zacharopoulos, E. Kolovou, A. Peppas, K. Koukoulakis, E. Bakeas, G. Schnakenburg, A. I. Philippopoulos, *Polyhedron* **2018**, *154*, 27.
- [26] R. Hodgkinson, V. Jurčík, H. Nedden, A. Blackaby, M. Wills, *Tetrahedron Lett.* **2018**, *59*, 930.
- [27] D. J. Braden, R. Cariou, J. W. Shabaker, R. A. Taylor, *Appl. Catal. A* **2019**, *570*, 367.
- [28] F. Durap, M. Aydemir, A. Baysal, D. Elma, B. Ak, Y. Turgut, *Inorg. Chim. Acta* **2014**, *411*, 77.
- [29] J. Volbeda, P. G. Jones, M. Tamm, *Inorg. Chim. Acta* **2014**, *422*, 158.
- [30] J. Chen, T. Zhang, X. Liu, L. Shen, *Catal. Lett.* **2019**, *149*, 601.
- [31] B. Qiu, W. Wang, X. Yang, *Catalysts* **2019**, *9*, 101.
- [32] S. Sultana, G. Borah, P. K. Gogoi, *Catal. Lett.* **2019**, *149*, 2142.
- [33] K. Z. Demmans, M. E. Olson, R. H. Morris, *Organometallics* **2018**, *37*, 4608.
- [34] W. Wu, T. Seki, K. L. Walker, R. M. Waymouth, *Organometallics* **2018**, *37*, 1428.
- [35] S. Sultana, G. Borah, P. K. Gogoi, *Appl. Organometal. Chem.* **2019**, *33*, e4595.
- [36] S. Konwer, A. Begum, S. Bordoloi, R. Boruah, *J. Polym. Res.* **2017**, *24*, 37.
- [37] K. Zhang, V. Dwivedi, C. Chi, J. Wu, *J. Hazard. Mater.* **2010**, *182*, 162.
- [38] M. S. Sher Shah, A. R. Park, K. Zhang, J. H. Park, P. J. Yoo, *ACS Appl. Mater. Interfaces* **2012**, *4*, 3893.
- [39] X. Yang, X. Zhang, Y. Ma, Y. Huang, Y. Wang, Y. Chen, *J. Mater. Chem.* **2009**, *19*, 2710.
- [40] F. Ahangaran, A. Hassanzadeh, S. Nouri, *Int. Nano Lett.* **2013**, *3*, 23.
- [41] W. Cheng, K. Tang, Y. Qi, J. Sheng, Z. Liu, *J. Mater. Chem.* **2010**, *20*, 1799.
- [42] I. Saikia, M. Hazarika, C. Tamuly, *Mater. Res. Express* **2016**, *3*, 105007.
- [43] S. Konwer, A. K. Guha, S. K. Dolui, *J. Mater. Sci.* **2013**, *48*, 1729.
- [44] C. Ma, K. Yang, L. Wang, X. Wang, *J. Appl. Biomater. Funct. Mater.* **2017**, *15*, 1.
- [45] P. M. Hallam, M. G. Mingot, D. K. Kampouris, C. E. Banks, *RSC Adv.* **2012**, *2*, 6672.
- [46] X. Wang, Y. Liu, H. Arandiyan, H. Yang, L. Bai, J. Mujtaba, Q. Wang, S. Liu, H. Sun, *Appl. Surf. Sci.* **2016**, *389*, 240.
- [47] M. N. Magubane, M. G. Alam, S. O. Ojwach, O. Q. Munro, *J. Mol. Struct.* **2017**, *1135*, 197.
- [48] N. U. D. Reshi, D. Senthurpandi, A. G. Samuelson, *J. Organometal. Chem.* **2018**, *866*, 189.
- [49] P. Bata, F. Notheisz, P. Kluson, A. Zsigmond, *Appl. Organometal. Chem.* **2015**, *29*, 45.
- [50] M. D. Bala, M. I. Ikhile, *J. Mol. Catal. A* **2014**, *385*, 98.
- [51] P. Bata, A. Zsigmond, M. Gyemant, A. Czegledi, P. Kluson, *Res. Chem. Intermed.* **2015**, *41*, 9281.
- [52] F. Wang, Z. Zhang, *ACS Sustainable Chem. Eng.* **2017**, *5*, 942.
- [53] M. N. Magubane, G. S. Nyamoto, S. O. Ojwach, O. Q. Munro, *RSC Adv.* **2016**, *6*, 65205.
- [54] J. Li, J. Liu, H. Zhou, Y. Fu, *Chem. Sus. Chem.* **2016**, *9*, 1339.
- [55] N. M. Patil, T. Sasaki, B. M. Bhanage, *ACS Sustainable Chem. Eng.* **2016**, *4*, 429.
- [56] R. Hudson, V. Chazelle, M. Bateman, R. Roy, C. J. Li, A. Moores, *ACS Sustainable Chem. Eng.* **2015**, *3*, 814.
- [57] B. S. Kumar, A. J. Amali, K. Pitchumani, *Mol. Catal.* **2018**, *448*, 153.

## SUPPORTING INFORMATION

Additional supporting information may be found online in the Supporting Information section at the end of this article.

**How to cite this article:** Sultana S, Bordoloi S, Konwer S, Borah G, Gogoi PK. Reduced graphene oxide/iron oxide hybrid composite material as an efficient magnetically separable heterogeneous catalyst for transfer hydrogenation of ketones. *Appl Organometal Chem.* 2020;e5582. <https://doi.org/10.1002/aoc.5582>